



## Landslide susceptibility mapping using GIS-Based-MCDM Method in Arabdagh forests of Iran

Ali Mastouri<sup>1\*</sup>, Shaban Shataee Jouibari<sup>2</sup>, Mohamad Hadi Moayeri<sup>3</sup>,  
Yasser Maghsoudi Mehrani<sup>4</sup> 

<sup>1</sup>PhD student, Department of Forestry, Faculty of Forest Sciences, Gorgan University of Agricultural Sciences and Natural Resources, Gorgan, Iran

<sup>2</sup>Professor, Department of Forestry, Faculty of Forest Sciences, Gorgan University of Agricultural Sciences and Natural Resources, Gorgan, Iran

<sup>3</sup>Associate Professor, Department of Forestry, Faculty of Forest Sciences, Gorgan University of Agricultural Sciences and Natural Resources, Gorgan, Iran

<sup>4</sup>Associate Professor, Department of Remote Sensing, University of KhajeNasir Tusi, Tehran, Iran

Article Info	Abstract
<b>Article type:</b> Research Article	Landslide hazards are relatively frequent in the mountainous regions of Northern Iran. This research aimed to utilize the potential application of a GIS-based multi-criteria decision-making model (MCDM) to evaluate and map landslide susceptibility in the Arabdagh forests, Golestan Province, Northern Iran. A ground truth landslide map including 78 points was prepared using aerial photographs and high-resolution satellite images and field surveys. The landslide influencing factors maps were produced and used as independent layers in the analysis. The landslide susceptibility map of the study area was produced by weighted linear combination (WLC) model based on AHP weights of factors. The resulting landslide susceptibility map was classified into five relative susceptibility zones according to the natural break method: very low, low, moderate, high, and very high with an area of 5.1%, 26.1%, 31.7%, 24.4%, and 12.8% of the total study area, respectively. The validation of the susceptibility map was performed using receiver operating characteristics (ROC) and area under the curve (AUC). The validation results showed an AUC of 0.852 (85.2%) with a standard error of 0.036. The susceptibility risk in the areas covered by shrub and herb where high and very high, respectively.
<b>Article history:</b> Received: <i>December 2021</i> Accepted: <i>November 2022</i>	
<b>Corresponding author:</b> a.m.forestry77@gmail.com	
<b>Keywords:</b> Landslide Susceptibility Multi-Criteria Decision Making (MCDM) AHP Arabdagh Forests	

**Cite this article:** Ali Mastouri, Shaban Shataee Jouibari, Mohamad Hadi Moayeri, Yasser Maghsoudi Mehrani. 2022. Landslide Susceptibility Mapping Using GIS-Based-MCDM Method In Arabdagh Forests of Iran. *Environmental Resources Research*, 10 (2), 165-182.



© The Author(s).

DOI: 10.22069/IJERR.2022.6298

Publisher: Gorgan University of Agricultural Sciences and Natural Resources

### Introduction

Natural hazards can result in many losses to properties and human life and wildlife (Feizizadeh and Blaschke, 2011). Landslides are a significant natural hazard (Skilodimou et al., 2018) that refer to a wide variety of processes that cause the downward and outward movement of slope-forming materials including rock, soil, artificial hill,

or a combination of these (Crosta and Clague, 2009). Landslides lead to damages to settlements, roads, forests, and agricultural fields and other infrastructures and cause casualties to the people living in the affected areas (Althuwaynee et al., 2012). Over the last decade, landslide incidences have increased (Kim et al., 2018) with their direct and indirect effects

including soil loss, damage to ecosystems, and destruction of forests (Kamranzad et al., 2015). Up until September 2007, about 4,900 landslides have been recorded and mapped in Iran causing a lot of damage (ILWP, 2007; Pourghasemi et al., 2013a). Various parameters cause a landslide that could be used to provide the landslide susceptibility zonation. Some of these parameters are topographic (Youssef et al., 2016), vegetation (Sarda and Pandey, 2019), soil (Jarjani et al., 2018), hydrological conditions (Kim et al., 2018), and geological parameters (Jarjani et al. 2018). Other parameters may as well play as triggering landslides, including heavy rainfall (Bera et al., 2019), and anthropogenic activities (Youssef et al., 2016). It is impossible to prevent the occurrence of natural disasters and disturbances. However, it is feasible to decrease the effects of natural hazards through proactive disaster mitigation planning and development of strategies and procedures (Ahmed et al., 2014). To reduce the damage caused by landslides, it is necessary to conduct a proper assessment of the potential damage due to landslides via an analysis of landslide-conditioning factors based on scientific knowledge and to pre-manage selected areas where landslides are expected (Oh et al., 2010). In fact, landslide hazard zonation (LHZ) is characterized as the division of land surface into homogeneous regions and their ranking to degrees of potential hazard resulted from the mass movement of land materials (Varnes, 1984; Guzzetti, 2005).

Recently, different studies have been conducted on landslide hazard assessment and modelling using GIS and RS capabilities and techniques (Pradhan and Youssef, 2010; Pradhan et al. 2010a; Bednarik et al., 2012; Mohammadi et al., 2012; Pourghasemi et al., 2013b; Devkota et al., 2013; Regmi et al., 2014; Cárdenas and Mera, 2016; Hadmoko et al., 2017; Stanley and Kirschbaum, 2017; Mahdadi et al., 2018; Kamranzad et al., 2015; Yilmaz, 2009). Moreover, since landslides are caused by different parameters, it is useful to create a landslide database using a Geospatial information system (GIS) (Oh et al., 2012). Using GIS as a basic analytical tool, in conjunction with

suitable models has facilitated the identification and mapping of landslides (Hong et al., 2018a; Hong et al., 2018b; Nsengiyumva et al., 2018; Alvioli et al., 2018). Numerous models and approaches have been applied for assessing landslide susceptibility which fall into four main groups: deterministic, heuristic, inventory-based probabilistic, and statistical techniques (Committee on the Review of the National Landslide Hazards Mitigation Strategy; 2004; Guzzetti et al., 1999). The heuristic approach applied in this research estimates the landslide potential from data on variables and their weights based on expert knowledge and opinions (Gupta and Joshi, 1990; Dahal et al., 2008b; Dahal et al., 2008a). The study area reported in this paper was formerly covered by deciduous broadleaf trees and almost half of it has been planted with coniferous species. Unfortunately, in recent years, this area has been severely affected by landslide damage, especially in the forested areas.

## Materials and Methods

### Study area

The study area, namely Arabdagh region is a mixed broadleaf and planted coniferous forest in the Golestan Province, Iran, with an area of 35 km<sup>2</sup> (Figure 1). This area was formerly a deciduous broadleaf forest. About fifty percent of the area was replanted with coniferous species between 1986 and 1991. The Arabdagh area is a hilly-mountainous region as part of the Alborz mountain range with an altitude of 140 to 1000 m above m.s.l. The average annual precipitation is 550 mm. The maximum slope in the area is 54°, with an average slope of 15°. According to the Central Office of Natural Resources and Watershed Management of Golestan Province (CONRWMGP), maximum and minimum precipitation occurs in February (99 mm) and May (28 mm), respectively. The major vegetation types are *Cupressus sempervirens var. horizontalis*, *Pinus pinea*, *Pinus sylvestris*, *Zelkova carpinifolia*, *Acer velutinum* and *Quercus castaneifolia* and about 78% of the area is covered with dense forest (Forest Silvicultural plan of Arabdagh area, 2016).

**Landslides**

Providing the occurred landslide distribution map is the first step (Pradhan et al. 2010b; Hong et al. 2017; Hong et al. 2016) for landslide susceptibility mapping. Therefore, several resources have been used for identification of landslide locations, including field surveys using GPS, interpretation of Google Earth satellite

images and pan-sharpened SPOT-6 imagery, and recorded landslide positions by Iranian Landslide Working Party (ILWP) and Forestry, Rangeland and Watershed Organization (FRWO). A number of 78 landslides were located in the Arabdagh region and saved as a point layer in GIS (Figure 1). Figure 2 is a picture of a landslide occurred in the study area.

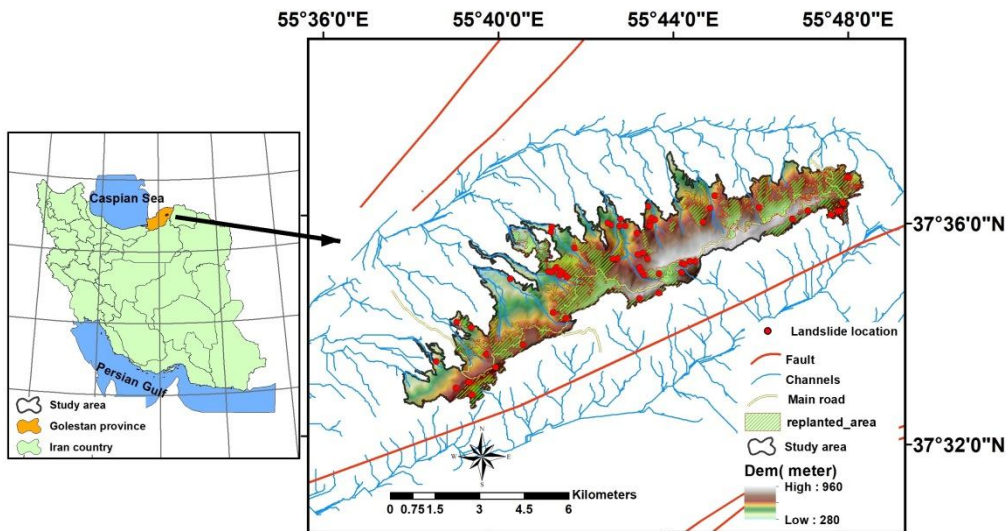


**Figure 1.** Location of the study area in the northern Iran and the distribution of the occurred landslides



**Figure 2.** A landslide occurred in the study area

**Landslide influencing factors**

Twenty-one factors affecting landslides including topographic (slope, aspect, elevation, profile curvature, plan curvature, surface roughness, and lineament density), vegetation (tree density, crown density, volume, and stand types), anthropogenic

conditions (distance to residential areas and roads), hydrological (drainage density, topographic wetness index (TWI), stream power index (SPI) and distance to rivers), soil (soil texture), climatic and meteorological parameters (average annual precipitation) and geology (distance to fault,

geology map) were selected and used for landslide analysis according to previous literature and landslide features. The identification of parameters causing landslide is the main step in the prediction of landslide susceptibility and risk assessment. The selection of landslide-conditioning parameters depends on different factors, like the nature and characteristics of the study area, landslide type, location, and scale of analysis, and previous knowledge of the main causes of landslides (Ayalew and Yamagishi, 2005). Additionally, in a GIS-based study, access to data is important and parameters should also be practical, complete, measurable, non-uniform, non-redundant, and well representing the whole study area (Ercanoglu and Gokceoglu, 2002). Accordingly, the main data were collected from different sources (Table 1) and saved in a spatial database. For each of

these landslide maps, the occurrence of landslides and their classes were determined.

SPOT-6 images (1.5 m) from the summer of 2018, Google Earth, and field sampling were also used to generate the vegetation land cover map. Topographic factors, topographic wetness index, and hydrologic factors were extracted from DEM with a spatial resolution of 12.5 m. Many researchers have considered Stream Power Index (SPI) and roughness factors as secondary topographical attributes computed from two or more primary topographic attributes (Althuwaynee et al., 2012). Some layers such as distance to residential areas, drainage, rivers, faults, and roads were mapped by the Euclidean distance tool at a grid size of 10×10 meters. In the study area, 21 parameters (Table 1) were selected for susceptibility analysis based on field surveys, landslide characteristics, and previous studies.

**Table 1.** Different data sources in the study area

Data	Description	Source
Digital Elevation Model (DEM)- 12.5 m	Download	<a href="https://earthexplorer.usgs.gov">https://earthexplorer.usgs.gov</a>
SPOT-6 Satellite Sensor (1.5m)	Bought	IMG_SPOT6_PMS_001_A: SPOT 6 2018-07-06:06:43:23.2 ORTHO PMS
Slope, Slope aspect, altitude, Curvature, Surface roughness, Topographic wetness index (TWI), Stream Power Index (SPI), river and Drainage Density	Extract	DEM
Fault and Geology	Digitized	Geological map of Gonbad 1:100.000
Road and Residential Area	Digitized	SPOT-6 Satellite and Google Earth
Tree density, Crown density and Volume	Interpolated	Field Sampling
Land Cover Type	Interpreted, field surveying	Visual interpretation of SPOT-6 satellite, Google Earth and field surveying
Soil texture	Digitized	Soil map of Gonbad, 1:63000
Rainfall	Interpolated	Synoptic gauges of Golestan province
Lineament density	extracted	SPOT-6 satellite
Landslide Location	Different sources	Historical Records, SPOT-6 Satellite, Google Earth and Field Sampling

### **Topographic factors**

Slope, aspect, elevation, curvature, surface roughness, and TWI factors were calculated from DEM. The slope is one of the most important factors for stability assessment (Bera et al., 2019). As the slope increases, the stress in soil or other unconsolidated material generally increases as well (Lee et al., 2004). Steep slopes with plan concave shapes are generally most susceptible to landslides (Knapen et al. 2006). The study area were classified into four categories, steep (>30°), high (20°–30°), moderately

high (10°–20°) and gentle (0°–10°). Aspect is related to parameters such as precipitation and sunlight exposure (Pradhan and Kim, 2014). An aspect map generally indicates the direction to which a mountain or hilly slope faces. In this study, the aspect of the slopes were divided into nine categories. Terrain elevation is an important factor to determine the landslide-prone areas and affects numerous biophysical and anthropogenic factors. Elevation values were divided into four categories using intervals of 200 m. The

curvature indicates the morphology of topography. Positive, negative, and zero values in profile curvatures indicate that the surface is upward convex, concave, and flat, respectively (Pourghasemi, 2016). It refers to the amount of slope or aspect variations in a specific direction (Wilson and Gallant, 2000). The profile curvature map was prepared in SAGA software. The surface roughness map quantifies topographic heterogeneity (Bièvre et al., 2016) and shows a factor that is commonly applied in the evaluation of landslide sensitivity (Abdulwahid and Pradhan, 2017). The surface roughness was prepared using Eq. (1) and reclassified into five classes using natural breaks (Jenks) (0–0.95, 0.95–1.82, 1.82–2.53, 2.53–3.46, 3.46–7).

$$(1) \quad \text{Topographic roughness} = (\text{Surface area}) / (\text{Planimetric area})$$

Lineament mapping is an important part of structural geology, and reveals the architecture of the underlying rock basement and help understand the causes of landslides (Ramli et al., 2010). The lineament extraction involves both manual visualization and automatic lineament extraction through software (Mwaniki et al., 2015). Various studies have been conducted on the application of filters (directional, Laplacian, and Sobel) on special bands or RGB satellite images to extract lineaments (Abdullah et al., 2013; Kavak, 2005; Hung et al. 2005). Lineament density was extracted from SPOT-6 images using the line density analyst extension and was classified into five categories.

#### **Anthropogenic factors**

Human activities strongly influence landslide susceptibility (Xing et al., 2014). Distance to roads and residential areas are considered as the main parameters, which increase the susceptibility to landslide via weakening of slope structure stability (Althuwaynee et al., 2012).

#### **Precipitation factor**

Rainfall is one of the main factors causing landslide (Sengupta et al., 2010; Claessens et al., 2007; Kwan et al., 2014). The rainfall distribution map was created for 21 years (1997–2018) of historical rainfall data collected from 6 gauge stations. The average annual precipitation intensity in the study area ranges from 440 to 650 mm. A higher amount of rainfall was found in the southeastern part of the study area. The statistical distribution of the accumulated average precipitation was prepared and was classified into five classes.

#### **Soil map**

Soil texture is an important factor that indirectly affects the whole environment of a particular area (Saklani, 2008). Soil characteristics affect the rate of water movement and the capacity of the soil to hold water. Soil physical features determine slope stability (Sidle and Ochiai, 2006). In the study area, three main types of soil texture were identified including Clay Loam, Silty Clay Loam, Clay, Clay Loam, and Rock. Soil texture layer was created by digitizing the soil texture map of the Golestan Province (1:100,000 scale) obtained from the Agriculture Department, Iran<sup>1</sup>.

#### **Hydrological factors**

Infiltration of rainfall into soil and run-off are significant factors affecting landslide occurrence (Pradhan and Kim, 2016). The proximity to drainage is another significant parameter for landslide susceptibility. In this study, the distance from the drainage map was classified into five categories. Drainage density is one of the main controlling factors of landslides because it changes the characteristic of the soil and its geotechnical properties (Pareta, 2004). Drainage density is the ratio of the total length of the stream to the area of the drainage basin. Drainage density is inversely related to the function of infiltration so that where drainage densities are higher, the movement of a surface flow

<sup>1</sup>(<http://jago.ir/HomePage.aspx?TabID=1&Site=Douran Portal &Lang=en-us>)

is faster (Cevik and Topal, 2003). The drainage density of the study area was classified into five categories. Another landslide-affecting topographic factor is TWI which is defined as  $\ln(A/\tan\beta)$ , where A is the upslope contributing area and  $\beta$  is the slope angle (Moore et al., 1991). TWI represents the spatial distribution of soil moisture (Pradhan and Kim, 2016). In this study, the TWI map was produced in SAGA-GIS software and divided into seven classes.

The stream power index (SPI) is a measure of the erosive power of water flow based on the assumption that discharge is proportional to the specific catchment area (Pradhan and Kim, 2016). Also, SPI is considered a factor resulting in stability (Kim et al., 2018). Higher SPI values cause an increased risk of slope erosion (Moore et al. 1991). In this study, the SPI was calculated from the slope and catchment area using the following equation (Eq. 2).

$$SPI = A_s * \tan B \quad (\text{Eq. 2})$$

where,  $A_s$  is the specific catchment area ( $m^2$ ) and B is the slope (in degrees).

### **Vegetation factors**

Impaired and converted land covers cause excessive damage from landslides and other natural hazards, while the presence of vegetation mitigates rainfall-induced landslide potential (Dahigamuwa et al., 2016). Besides topographic, lithological, and hydrological characteristics, the vegetation cover can improve the stability of the slope by mechanically reinforcing the soil and positively influencing its water balance. Landslide susceptibility is decreased in stands with smaller distances from trees and where gap lengths are small (Moos et al. 2016). Some researchers have proven the positive influences of forest characteristics such as vegetation density on landslide assessment (Vergani et al., 2012; Mao et al., 2014). The Arabdagh area has 12 vegetation cover types: *Cupressus sempervirens var horizontalis*, *Cupressus arizonica*, *Pinus brutia*, *Pinus pinea*, *Pinus sylvestris*, *Zelkova carpinifolia*, *Carpinus betulus*, mixed hardwood, mixed softwood,

mixed hardwood and softwood, agricultural area, and herb-shrub areas. Other vegetation factors such as volume, crown cover, and tree density were measured in the field and interpolated to the whole area using the Kriging method and classified in the specified categories.

### **Geological factors**

Landslides are greatly affected by the lithological properties of a land surface (Pradhan and Kim, 2016). The lithology map and fault lineaments were digitized and extracted from the 1:100000 geological map. Geologically, the Arabdagh area consists of two lithological formations, including JMZ and GAL. JMZ Formation consists of grey thick-bedded limestone and dolomite and QAL formation comprises stream and braided channel and flood plain deposits. The fault is another factor that affects resistance-related elements of bedrock (Chen et al., 2017). It has a close relationship with slope instability (Dai and Lee 2002). The likelihood of occurrence of landslides is related to the distance from faults (Pradhan and Lee, 2010a). The distance to fault map was divided into ten categories.

### **Susceptibility mapping**

We used the analytical hierarchy process (AHP) to derive weights of the factors. In the process, relative rating values ranged from 0 to 9, which were considered for subclasses of the layers, where higher rating represents a higher effect on landslide occurrence. Computing weights for the landslide conditioning maps is a basic requirement multi-criteria decision making (MCDM) (Parsons and Frost, 2000). In fact, AHP is used to acquire a priority scale for factors when handling multi-criteria decisions (Pourghasemi et al., 2012). Decomposition, comparative decision, and a combination of priorities are the main principles of AHP (Basu and Pal, 2017). This procedure has been widely used in different fields such as site selection, suitability analysis, and landslide susceptibility mapping (Ayalew et al., 2005; Hasekiogulları and Ercanoglu, 2012).

The standard scale for using the AHP method has been given in Table 3, where value 3 is assigned to the class with the least influence, and value 9 is assigned to the class with the maximum influence. Since an expert’s judgment can violate the transitivity rule and thus result in an inconsistency, the consistency ratio (CR) is used to check the consistency of the comparison matrix and CR (Eq. 3 and 4) values below 0.1 are considered acceptable (Ayalew et al., 2004).

$$CR = \frac{CI}{RI} \tag{3}$$

where CI (Eq. 4) is the consistency index calculated as:

$$CI = \frac{\lambda_{max} - n}{n - 1} \tag{4}$$

where n is the order of the matrix and max is the major value of the matrix.

Random index (RI) was derived from a sample of randomly generated reciprocal matrices and is dependent on the size of the matrix as given in (Table 2).

**Table 2.** Random index value (Saaty, 1990)

n	1	2	3	4	5	6	7	8	9	10
RI	0.0	0.0	0.58	0.90	1.12	1.24	1.32	1.41	1.45	1.51

After preparing map of layers affecting landslide and calculating their weights using AHP (Table 3), the layers were combined through weighted linear

combination method (WLC) to generate the landslide susceptibility map using Eq. 5.

$$LSI = \sum_{i=1}^n R_i * W_i \tag{5}$$

**Table 3.** Scales for pairwise comparisons (Saaty, 2005, 1977)

Intensity of Importance	Description
1	Equal importance
3	Moderate importance
5	Strong or essential importance
7	Very strong or demonstrated importance
9	Extreme importance
2, 4, 6, 8	Intermediate values
Reciprocals	Value for inverse comparison

In equation 5, LSI represents the final score, Ri is the rating classes, Wi is the weight for each landslide-conditioning factor and n is the number of landslide factors (Gorsevski et al., 2006a).

The WLC technique is a popular method that is applicable and appropriate for the flexible combination of qualitative and quantitative thematic layers and is one of the most commonly used GIS-MCDA method (Feizizadeh and Blaschke, 2013). It is also one of the most used decision models for landslide susceptibility and natural hazard zoning and mapping due to its reliance on expert knowledge.

The map derived through WLC was divided into five susceptibility categories (very low, low, moderate, high, and very high) based on the natural break method.

The validation step is an essential stage in evaluating the accuracy of the susceptibility map. For this we used the receiver operating characteristic (ROC) curve and area under the curve (AUC) (Roodposhti et al., 2014; El Jazouli et al., 2019; Guo et al., 2015). This is achieved through comparing the map obtained from the WLC and the landslide inventory map. The AUC of the ROC curve supplies a diagnosis that can be used as a statistical measurement of the performance.

The AUC value of the ROC curve, ranging from 0.5 to 1.0, is a numeric index of map accuracy (Holsinger et al., 2016). In some studies, the AUC has been divided into five qualitative categories, including excellent (0.9–1.0), good (0.8–0.9), fair (0.7–0.8), poor (0.6–0.7), and fail (<0.6),

which is represented by the diagonal straight line (Vakhshoori and Zare, 2016).

The methodological flowchart of the study is presented in Figure 3.

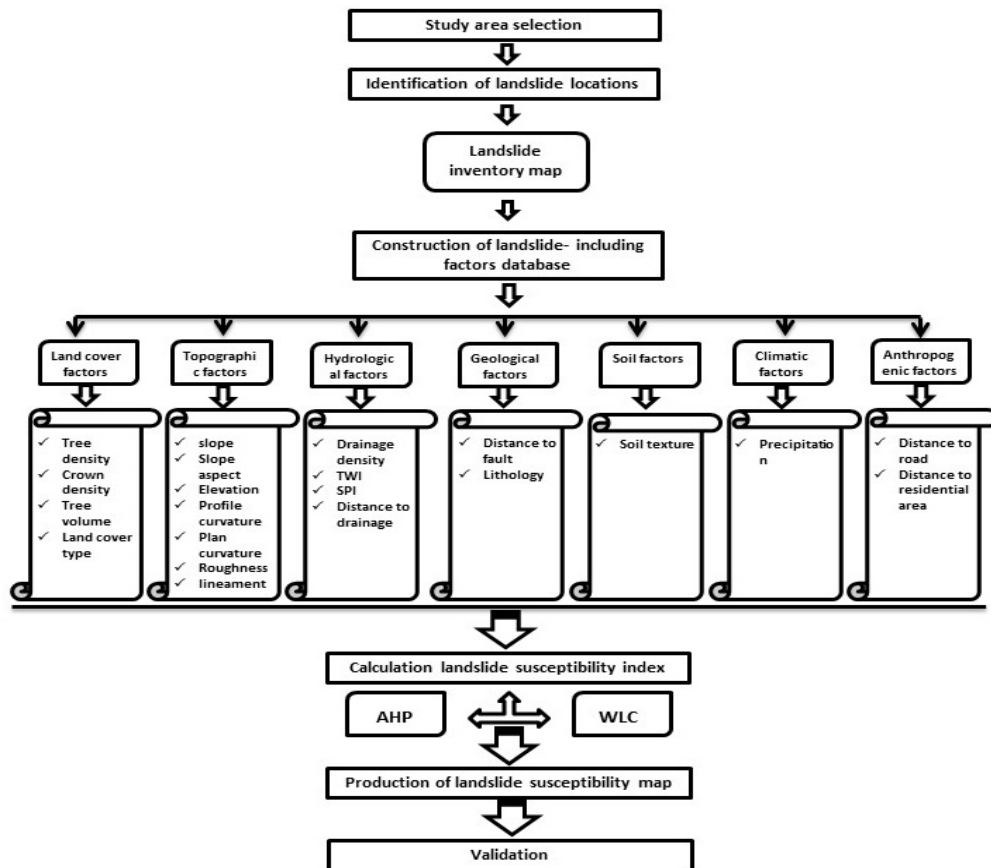


Figure 3. Flowchart of the study

**Results and Discussions**

In this study, a GIS-based AHP as a multi-criteria evaluation approach (MCE) was used to develop a landslide susceptibility map for the Arabdagh area. To achieve this objective, 21 landslide inducing variables were employed, namely topographic factors (slope, slope aspect, elevation, plan and profile curvatures, surface roughness, and lineament density), hydrological factors (drainage density, topographic wetness index (TWI), stream power index (SPI) and distance to rivers), climatic and meteorological parameters (mean annual precipitation), vegetation factors (crown density, tree density, volume and vegetation type), anthropogenic conditions (distance to residential areas and

distance to road), soil factor (soil texture), and geology parameters (distance to fault, lithology, and geology). The AHP is a multi-criterion decision-making approach that allows factors to be weighted and performed in the decision-making process (Bera et al., 2019; Feizizadeh and Blaschke, 2013). The resulting pairwise comparison matrix for the groups and contributing factors and their relative weights were extracted from AHP analysis based on expert judgments (Table 4). Accordingly, the slope, volume, drainage density, distance to faults, and roads were the most important landslide causative factors, respectively. The resulting consistency ratios (CR) were acceptable for the groups and factors.



**Table 4.** Scales for pairwise comparisons (Saaty, 1990; Roodposhti et al. 2014)

Group	Causative factors	Normalized weight values
Topographic	Elevation	0.0279
	Slope	0.4103
	Slope aspect	0.2136
	Profile curvature	0.1283
	Plan curvature	0.0605
	Surface roughness	0.1213
	Lineament density	0.0381
		Consistency Ratio (CR)=0.05
Hydrology	Distance to river	0.06
	Drainage density	0.5286
	TWI	0.2643
	SPI	0.1471
		Consistency Ratio (CR)=0.01
Soil type	Soil type	Consistency Ratio (CR)=0
Land cover	Forest type	0.2754
	Volume	0.5495
	Tree density	0.1134
	Crown closure	0.0618
		Consistency Ratio (CR)=0.08
Geology	Geology	0.358
	Distance to fault	0.642
		Consistency Ratio (CR)=0
Climatic and meteorological	Average annual precipitation	Consistency Ratio (CR)=0
Anthropogenic	Distance to residential area	0.35
	Distance to road	0.65
		Consistency Ratio (CR)=0
<b>Main groups</b>		
Topographic		0.3543
Hydrology		0.2399
Soil type		0.1587
Land cover		0.1036
Geology		0.0676
Climatic and meteorological		0.448
Anthropogenic		0.0312
		Consistency Ratio (CR)=0.02

Landslide-inducing thematic layers were integrated using weights of groups, factors, and sub-classes determined by experts using the AHP method to produce the landslide susceptibility map. The weighted map was classified into five susceptibility categories such as very low (2.2–3.6), low (3.6–4.2), moderate (4.2–4.7), high (4.7–5.2), and very high (5.2–6.7) based on the natural break classifier method (Figure. 4). The area percentages of each class are displayed in Figure 5.

Very low, low, and moderate landslide susceptible areas represented 5.1%, 26.1%, and 31.7% of the total study area, respectively. Figure 18 demonstrates that 37.2% (1317.32 ha) of the study area has high- to very high landslide hazard potential. Therefore, the moderate susceptibility class accounts for the largest area (31.7%), based on the landslide susceptibility map (Figure 10). The landslide vulnerability is in the

west, northeast, and Northwest parts of the study area near drainage network (0–400 m). These results follow closely findings of other studies (Ahmadi et al. 2005; Mohammadi and Pourghasemi, 2017). Our results can be attributed to the high humidity in the north and west of the study area. Most of the high and very high zones of the landslide potential map included slopes between 10 and 30 degrees. Low and high slopes have no significant effect on landslide occurrence due to reduced gravity force and decreased soil depth, respectively. Higher susceptible areas were found in altitudes between 400 m and 600 m followed by 600 m and 800 m occupying 30.5% and 42.25% of the total area, respectively. The elevation influences on vegetation structure and air humidity in the curvatures, convex and concave classes demonstrate higher vulnerability than the flat areas.

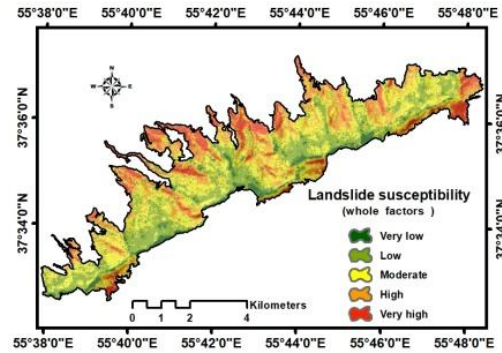


Figure 4. The landslide susceptibility map

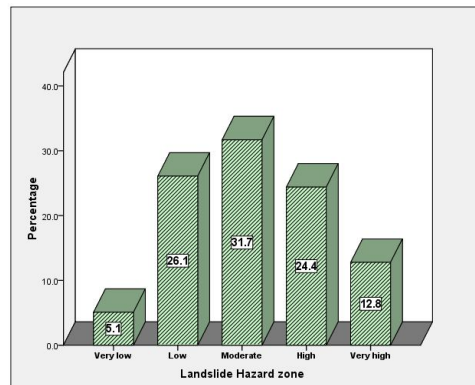


Figure 5. The percentages of each class of the landslide susceptibility map in the study area

These surfaces are always exposed to rain and other climatic conditions that loosen the soil (Oh et al., 2009). In the case of roughness, the values between 1 and 7 refers to lower and higher topographic roughness in the study area, and the values between 2.5 and 3.5 indicate the most vulnerable classes for landslide susceptibility. In terms of distance from the fault, road, and residential areas, the very high landslide-prone classes are located in the near to medium distances, indicating the direct impact of land activities and anthropogenic interventions on landslide occurrence, respectively. The farther the distance from the fault and road, the lower the landslide risk probability. Some studies (Oh et al., 2009; Lee and Pradhan, 2007) have shown the inverse relationship between the distance from the fault and landslide susceptibility. SPI represents the material viscosity and the topography steepness (Althuwaynee et al., 2012). In this study, the values between 1.6 and 3.7 demonstrate areas with high capability for

landslide. A higher probability of landslide is obtained in areas with class QL in the geology map. This may be due to the dominant area of this class (80%). The soil texture with three classes showed that “Clay loam, Silty Clay Loam” soil texture classes were more inclined to landslide. Regarding forest characteristics including tree density, canopy density, volume, and type of vegetation cover, the highest landslide risk was obtained in classes 25.4–527.5 and 750–964, 37–51 and 63–74 percent, 0–120.3 cubic meter/ha, and herb and shrub lands, respectively. Forest variables reduce the likelihood of landslide risk. Rainfall is a landslide-triggering factor strongly influenced by the landscape and other specific environmental factors and leads to slope instability. Finally, class 2–3.3 km/km<sup>2</sup> in lineament factor, class 3–3.9 km/km<sup>2</sup> in drainage density map and class 5.3–6.3 in TWI factor were very prone to landslide occurrence. For drainage density and TWI, landslide susceptibility values showed that when drainage density and

TWI increased, the probability of landslide increased too. To determine the accuracy of the landslide potential map, the map obtained from the WLC method and that of the landslide inventory were compared

through the receiver operating characteristic (ROC) curve and area under the curve (AUC). The results showed 85.2% accuracy with a standard error of 0.036 for the WLC method (Figure 6).

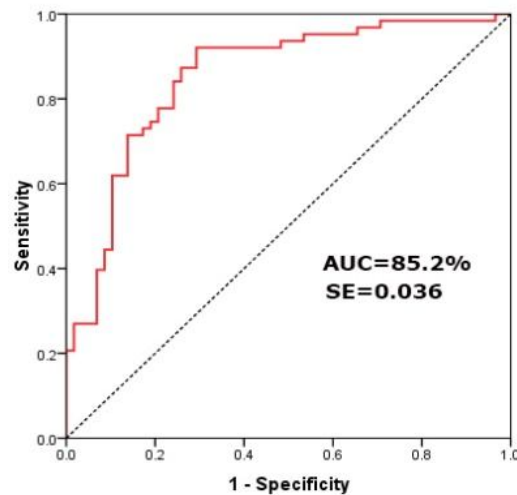


**Figure 6.** Receiver operating characteristic (ROC) curve of the landslide susceptibility map using the inventory data set

### Conclusion

Landslide is an important natural phenomenon which has both direct and indirect impacts on people's livelihood and natural resources and brings about damaging consequences. The recognition of areas with a high probability of landslide risk and its mapping is the interests of responsible organizations and comprises the aims of this study. We used a GIS-Based multi-criteria decision analysis as a heuristic model, to develop a landslide susceptibility map with a case study of the Arabdagh area, Iran. This area is susceptible to frequent landslide occurrences, especially in years when the intensity of rainfall is high. To achieve this objective, the relative weights of the conditioning factors and their categories were extracted using AHP based on expert opinion and pairwise comparison matrix. Then the factors were combined using Weighted Linear Combination (WLC) method. Eventually, the performance of the model was validated using the receiver operating characteristic (ROC) curve and the area under curve (AUC). The AUC value of 85.2% indicated good accuracy of the landslide assessment and demonstrates

that the selected landslide causing factors has been performed correctly. The resulting landslide susceptibility map was classified into five relative susceptibility zones according to the natural break method: very low, low, moderate, high, and very high with an area of 5.1%, 26.1%, 31.7%, 24.4%, and 12.8%, respectively. Results showed that approximately 60.3% of the landslide's inventory points were located in the high and very high susceptibility zones. According to the classified landslide map, the susceptibility risk in the north and partly in the southern parts of the study area mainly represented by shrub and herb lands with high and very high values. The rest of the area with very low to moderate landslide vulnerability values covers the middle part of the study area, where the endemic broadleaf species and planted coniferous trees are established with high values of forest characteristics such as volume, canopy cover percentage, and tree density. The results of this research could be useful for forest managers in decision-making and forestry plans management, land-use planning, and supporting efforts for mitigation of future landslide hazards.

## References

- Abdullah, A., Nassr, S., and Ghaleeb, A. 2013. Remote Sensing and Geographic Information System for Fault Segments Mapping a Study from Taiz Area, Yemen. *Journal of Geological Research*. 2013, 1-12.
- Abdulwahid, W.M., and Pradhan, B. 2017. Landslide vulnerability and risk assessment for multi-hazard scenarios using airborne laser scanning data (LiDAR). *Landslides*. 14(3), 1057-1076.
- Ahmadi, E., Dervish, A., Makhdoom, M. and Abolqasemi, S. 2005. Road routing based on environmental GIS principles. *Geomatics Conference*. 84, 8 pp.
- Ahmed, M.F., Rogers, J.D., and Ismail, E.H. 2014. A regional level preliminary landslide susceptibility study of the upper Indus river basin. *European Journal of Remote Sensing*. 47(1), 343-373.
- Althuwaynee, O.F., Pradhan, B., and Lee, S. 2012. Application of an evidential belief function model in landslide susceptibility mapping. *Computers & Geosciences*. 44, 120-135.
- Alvioli, M., Melillo, M., Guzzetti, F., Rossi, M., Palazzi, E., Von Hardenberg, J., and Peruccacci, S. 2018. Implications of climate change on landslide hazard in Central Italy. *Science of the Total Environment*. 630, 1528-1543.
- Ayalew, L., and Yamagishi, H. 2005. The application of GIS-based logistic regression for landslide susceptibility mapping in the Kakuda–Yahiko Mountains, Central Japan. *Geomorphology*. 65, 15-31.
- Ayalew, L., Yamagishi, H., and Ugawa, N. 2004. Landslide susceptibility mapping using GIS-based weighted linear combination, the case in Tsugawa area of Agano River, Niigata Prefecture, Japan. *Landslides*. 1(1), 73-81.
- Ayalew, L., Yamagishi, H., Marui, H., and Kanno, T. 2005. Landslides in Sado Island of Japan: Part II. GIS-based susceptibility mapping with comparisons of results from two methods and verifications. *Engineering Geology*. 81(4), 432-445.
- Basu, T., and Pal, S. 2017. Exploring landslide susceptible zones by analytic hierarchy process (AHP) for the Gish River Basin, West Bengal, India. *Spatial Information Research*. 25(5), 665-675.
- Bednarik, M., Yilmaz, I., and Marschalko, M. 2012. Landslide hazard and risk assessment: a case study from the Hlohovec–Sered’ landslide area in south-west Slovakia. *Natural Hazards*. 64(1), 547-575.
- Bera, A., Mukhopadhyay, B.P., and Das, D. 2019. Landslide hazard zonation mapping using multi-criteria analysis with the help of GIS techniques: a case study from Eastern Himalayas, Namchi, South Sikkim. *Natural Hazards*. 96(2), 935-959.
- Bièvre, G., Jongmans, D., Goutaland, D., Pathier, E., and Zumbo, V. 2016. Geophysical characterization of the lithological control on the kinematic pattern in a large clayey landslide (Avignonet, French Alps). *Landslides*. 13(3), 423-436.
- Cárdenas, N.Y., and Mera, E.E. 2016. Landslide susceptibility analysis using remote sensing and GIS in the western Ecuadorian Andes. *Natural Hazards*. 81(3), 829-1859.
- Cevik, E., and Topal, T. 2003. GIS-based landslide susceptibility mapping for a problematic segment of the natural gas pipeline, Hendek (Turkey). *Environmental Geology*. 44(8), 949-962.
- Chen, W., Panahi, M., and Pourghasemi, H.R. 2017. Performance evaluation of GIS-based new ensemble data mining techniques of adaptive neuro-fuzzy inference system (ANFIS) with genetic algorithm (GA), differential evolution (DE), and particle swarm optimization (PSO) for landslide spatial modelling. *Catena*. 157, 310-324.
- Claessens, L., Knapen, A., Kitutu, M.G., Poesen, J., and Deckers, J.A. 2007. Modelling landslide hazard, soil redistribution and sediment yield of landslides on the Ugandan footslopes of Mount Elgon. *Geomorphology*. 90(1-2), 23-35.
- Committee on the Review of the National Landslide Hazards Mitigation Strategy. 2004. Partnerships for reducing landslide risk. Assessment of the National landslide hazards mitigation strategy. Board on Earth Sciences and Resources, Division on earth and life studies, The National Academic Press, Washington, p 143.

- Crosta, G., and Clague, J. 2009. Dating, triggering, modeling and hazard assessment of large landslides. *Geomorphology*. 103, 1-4.
- Dahal, R.K., Hasegawa, S., Nonomura, A., Yamanaka, M., Dhakal, S., and Paudyal, P. 2008<sup>a</sup>. Predictive modelling of rainfall-induced landslide hazard in the Lesser Himalaya of Nepal based on weights-of-evidence. *Geomorphology*. 102(3-4), 496-510.
- Dahal, R.K., Hasegawa, S., Nonomura, A., Yamanaka, M., Masuda, T., and Nishino, K. 2008<sup>b</sup>. GIS-based weights-of-evidence modelling of rainfall-induced landslides in small catchments for landslide susceptibility mapping. *Environmental Geology*. 54(2), 311-324.
- Dahigamuwa, T., Yu, Q., and Gunaratne, M. 2016. Feasibility study of land cover classification based on normalized difference vegetation index for landslide risk assessment. *Geosciences*. 6(4), 45: <https://doi.org/10.3390/geosciences6040045>.
- Dai, F.C., and Lee, C.F. 2002. Landslide characteristics and slope instability modeling using GIS, Lantau Island, Hong Kong. *Geomorphology*. 42(3-4), 213-228.
- Devkota, K.C., Regmi, A.D., Pourghasemi, H.R., Yoshida, K., Pradhan, B., Ryu, I.C., Dhital, M.R., and Althuwaynee, O.F. 2013. Landslide susceptibility mapping using certainty factor, index of entropy and logistic regression models in GIS and their comparison at Mugling–Narayanghat road section in Nepal Himalaya. *Natural Hazards*. 65(1), 135-165.
- El Jazouli, A., Barakat, A., and Khellouk, R. 2019. GIS-multi criteria evaluation using AHP for landslide susceptibility mapping in Oum Er Rbia high basin (Morocco). *Geoenvironmental Disasters*, 6(1), 1-12.
- Ercanoglu, M., and Gokceoglu, C. 2002. Assessment of landslide susceptibility for a landslide-prone area (north of Yenice, NW Turkey) by fuzzy approach. *Environmental Geology*. 41, 720-730.
- Feizizadeh, B., and Blaschke, T. 2011. Landslide risk assessment based on GIS multi-criteria evaluation: a case study in Bostan-Abad County, Iran. *Journal of earth science and engineering*. 1(1), 66-77.
- Feizizadeh, B., and Blaschke, T. 2013. GIS-multi criteria decision analysis for landslide susceptibility mapping: comparing three methods for the Uremia lake basin, Iran. *Natural Hazards*. 65(3), 2105-2128.
- Gorsevski, P.V., Jankowski, P., and Gessler, P.E. 2006<sup>a</sup>. An heuristic approach for mapping landslide hazard by integrating fuzzy logic with analytic hierarchy process. *Control and Cybernetics*. 35, 121-146.
- Gorsevski, P.V., Gessler, P.E., Foltz, R.B., and Elliot, W.J. 2006<sup>b</sup>. Spatial prediction of landslide hazard using logistic regression and ROC analysis. *Transactions in GIS*. 10(3), 395-415.
- Guo, C., Montgomery, D.R., Zhang, Y., Wang, K., and Yang, Z. 2015. Quantitative assessment of landslide susceptibility along the Xianshuihe fault zone, Tibetan Plateau, China. *Geomorphology*. 248, 93-110.
- Gupta, R.P., and Joshi, B.C. 1990. Landslide hazard zoning using the GIS approach—a case study from the Ramganga catchment, Himalayas. *Engineering Geology*. 28(1-2), 119-131.
- Guzzetti, F. 2005. Review and selection of optimal geological models related to spatial information available, Action 1.14 Risk-aware is partially co-financed by the European Union under the INTEREG IIIB CADSES program, 44 pp.
- Guzzetti, F., Carrara, A., Cardinali, M., and Reichenbach, P. 1999. Landslide hazard evaluation: a review of current techniques and their application in a multi-scale study, Central Italy. *Geomorphology*. 31 (1–4), 181-216.
- Hadmoko, D.S., Lavigne, F., and Samodra, G. 2017. Application of a semiquantitative and GIS-based statistical model to landslide susceptibility zonation in Kayangan Catchment, Java, Indonesia. *Natural Hazards*. 87(1), 437-468.
- Hasekioğulları, G.D., and Ercanoglu, M. 2012. A new approach to use AHP in landslide susceptibility mapping: a case study at Yenice (Karabuk, NW Turkey). *Natural Hazards*. 63(2), 1157-1179.
- He, Y., and Beighley R.E. 2008. GIS-based regional landslide susceptibility mapping: A case study in southern California. *Earth Surface Processes and Landforms*. 33, 380-393.

- Holsinger, L., Parks, S.A., and Miller, C. 2016. Weather, fuels, and topography impede wildland fire spread in western US landscapes. *Forest Ecology and Management*. 380, 59-69.
- Hong, H., Liu, J., Bui, D.T., Pradhan, B., Acharya, T.D., Pham, B.T., and Ahmad, B.B. 2018<sup>a</sup>. Landslide susceptibility mapping using J48 Decision Tree with AdaBoost, Bagging and Rotation Forest ensembles in the Guangchang area (China). *Catena*. 163, 399-413.
- Hong, H., Pradhan, B., Sameen, M.I., Kalantar, B., Zhu, A., and Chen, W. 2018<sup>b</sup>. Improving the accuracy of landslide susceptibility model using a novel region-partitioning approach. *Landslides*. 15(4), 753-772.
- Hong, H., Naghibi, S.A., Pourghasemi, H.R., and Pradhan, B. 2016. GIS-based landslide spatial modeling in Ganzhou City, China. *Arabian Journal of Geosciences*. 9(2), 112-137.
- Hong, H., Chen, W., Xu, C., Youssef, A.M., Pradhan, B., and Tien Bui, D. 2017. Rainfall-induced landslide susceptibility assessment at the Chongren area (China) using frequency ratio, certainty factor, and index of entropy. *Geocarto International*, 32(2), 139-154.
- Hung, L.Q., Batelaan, O., and De Smedt, F. 2005. Lineament extraction and analysis, comparison of Landsat-ETM and ASTER imagery, Case study: Suoimuoi tropical karst catchment, Vietnam. In *Proceedings of SPIE Remote Sensing for Environmental Monitoring, GIS Applications and Geology*, M. Ehlers, and U. Michel, eds. (International Society for Optics and Photonics), p 12.
- Iranian Landslide Working Party (ILWP). 2007. Iranian landslides list. Forest, Rangeland, and Watershed Association, Iran. 60 p.
- Jarjani, A., Akbari, H., Hosseini, S.A., and Abdi, O. 2018. Investigation of landslide danger zoning using analytical hierarchy process in GIS environment (case study: Azadshahr Kohmian forestry design). *Journal of Watershed Management Research*. 10(18), 197-207.
- Kamranzad, F., Mohasel Afshar, E., Mojarb, M., and Memarian, H. 2015. Landslide hazard zonation in Tehran province using data-driven and AHP methods. *Scientific Quarterly Journal*. 25(97), 101-114.
- Kavak, K.S. 2005. Determination of palaeotectonic and neotectonic features around the Menderes Massif and the Gediz Graben (West. Turkey) using Landsat TM image. *International Journal of Remote Sensing*. 26, 59-78.
- Kim, J.C., Lee, S., Jung, H.S., and Lee, S. 2018. Landslide susceptibility mapping using random forest and boosted tree models in Pyeong-Chang, Korea. *Geocarto International*. 33(9), 1000-1015.
- Knapen, A., Kitutu, M.G., Poesen, J., Breugelmans, W., Deckers, J., and Muwanga, A. 2006. Landslides in a densely populated county at the footslopes of Mount Elgon (Uganda): characteristics and causal factors. *Geomorphology*. 73(1-2), 149-165.
- Kwan, J.S., Chan, S.L., Cheuk, J.C., and Koo, R.C.H. 2014. A case study on an open hillside landslide impacting on a flexible rockfall barrier at Jordan Valley, Hong Kong. *Landslides*. 11(6), 1037-1050.
- Le, Q.H., Van Nguyen, T.H., Do, M.D., Le, T.C.H., Nguyen, H.K., and Luu, T.B. 2018. TXT-tool 1.084-3.1: landslide susceptibility mapping at a regional scale in Vietnam. In *Landslide dynamics: ISDR-ICL landslide interactive teaching tools* (pp. 161-174). Springer, Cham.
- Lee, S., Choi, J., and Min, K. 2004. Probabilistic landslide hazard mapping using GIS and remote sensing data at Boun, Korea. *International Journal of Remote Sensing*. 25(11), 2037-2052.
- Lee, S., Ryu, J., Lee, M., and Won, J. 2003. Landslide susceptibility analysis using the artificial neural network at Boun, Korea. *Environ Geol*. 44, 820-833.
- Lee, S., and Pradhan, B. 2007. Landslide hazard mapping at Selangor, Malaysia using frequency ratio and logistic regression models. *Landslides*. 4 (1), 33-41.
- Mahdadi, F., Boumezbeur, A., Hadji, R., Kanungo, D.P., and Zahri, F. 2018. GIS-based landslide susceptibility assessment using statistical models: a case study from Souk Ahras province, NE Algeria. *Arabian Journal of Geosciences*. 11(17), 476.
- Mao, Z., Bourrier, F., Stokes, A., and Fourcaud, T. 2014. Three-dimensional modeling of slope stability in heterogeneous montane forest ecosystems. *Ecological Modelling*. 273, 11-22.

- Mohammadi, M., and Pourghasemi, A. 2017. Prioritization of landslide-conditioning factors and its landslide susceptibility mapping using random forest new algorithm. *Journal of Watershed Management Research*. 8(15), 161-170.
- Mohammadi, M., Pourghasemi, H.R., and Pradhan, B. 2012. Landslide susceptibility mapping at Golestan Province, Iran: a comparison between frequency ratio, Dempster–Shafer, and weights-of-evidence models. *Journal of Asian Earth Sciences*. 61, 221-236.
- Moore, I.D., Grayson, R.B., and Ladson, A. 1991. Digital terrain modeling: a review of hydrological, geomorphological, and biological applications. *Hydrology Process*. 5, 3-30.
- Moos, C., Bebi, P., Graf, F., Mattli, J., Rickli, C. and Schwarz, M. 2016. How does forest structure affect root reinforcement and susceptibility to shallow landslides? *Earth Surface Processes and Landforms*. 41(7), 951-960.
- Mwaniki, M.W., Moeller, M.S., and Schellmann, G. 2015. A comparison of Landsat 8 (OLI) and Landsat 7 (ETM+) in mapping geology and visualizing lineaments: A case study of central region Kenya. *International Archives of the Photogrammetry, Remote Sensing & Spatial Information Sciences*.
- Nsengiyumva, J.B., Luo, G., Nahayo, L., Huang, X., and Cai, P. 2018. Landslide susceptibility assessment using spatial multi-criteria evaluation model in Rwanda. *International journal of Environmental Research and Public Health*. 15(2), 243.
- Oh, H.J., Lee, S., and Soedradjat, G.M. 2010. Quantitative landslide susceptibility mapping at Pemalang area, Indonesia. *Environmental Earth Sciences*. 60(6), 1317-1328.
- Oh, H.J., Park, N.W., Lee, S.S. and Lee, S. 2012. Extraction of landslide-related factors from ASTER imagery and its application to landslide susceptibility mapping. *International Journal of Remote Sensing*. 33(10), 3211-3231.
- Oh, H.J., Lee, S., Chotikasathien, W., Kim, C.H., and Kwon, J.H. 2009. Predictive landslide susceptibility mapping using spatial information in the Pechabun area of Thailand. *Environmental Geology*. 57(3), 641-651
- Pareta, K. 2004. Hydro-geomorphology of Sagar district (MP): a study through remote sensing technique. In: *Proceeding in XIX MP young scientist congress, Madhya Pradesh council of science and technology (MAPCOST), Bhopal*.
- Parsons, R.L., and Frost, J.D. 2000. Interactive analysis of spatial subsurface data using GIS-based tool. *Journal of Computing in Civil Engineering*. 14(4), 215-222.
- Pourghasemi, H.R., Moradi, H.R., and Aghda, S.F. 2013<sup>a</sup>. Landslide susceptibility mapping by binary logistic regression, analytical hierarchy process, and statistical index models and assessment of their performances. *Natural Hazards*. 69(1), 749-779.
- Pourghasemi, H.R., Pradhan, B., Gokceoglu, C., Mohammadi, M., and Moradi, H.R. 2013<sup>b</sup>. Application of weights-of-evidence and certainty factor models and their comparison in landslide susceptibility mapping at Haraz watershed, Iran. *Arabian Journal of Geosciences*. 6(7), 2351-2365.
- Pourghasemi, H.R., Pradhan, B., and Gokceoglu, C. 2012. Application of fuzzy logic and analytical hierarchy process (AHP) to landslide susceptibility mapping at Haraz watershed, Iran. *Natural Hazards*. 63(2), 965-996.
- Pourghasemi, H.R. 2016. GIS-based forest fire susceptibility mapping in Iran: a comparison between evidential belief function and binary logistic regression models. *Scandinavian Journal of Forest Research*. 31(1), 80-98.
- Pradhan, B., and Lee, S. 2010<sup>a</sup>. Delineation of landslide hazard areas on Penang Island, Malaysia, by using frequency ratio, logistic regression, and artificial neural network models. *Environment Earth Science*. 60(5), 1037–1054.
- Pradhan, B., and Lee, S. 2010<sup>b</sup>. Regional landslide susceptibility analysis using back-propagation neural network model at Cameron Highland, Malaysia. *Landslides*. 7:1330.
- Pradhan, B. and Youssef, A.M. 2010. Manifestation of remote sensing data and GIS on landslide hazard analysis using spatial-based statistical models. *Arabian Journal of Geoscience*. 3(3), 319-326.

- Pradhan, B., Youssef, A.M., and Varathrajoo, R. 2010<sup>a</sup>. Approaches for delineating landslide hazard areas using different training sites in an advanced artificial neural network model. *Geospatial Information Science*. 13(2), 93-102
- Pradhan, B., Lee, S., and Buchroithner, M.F. 2010<sup>b</sup>. Remote sensing and GIS-based landslide susceptibility analysis and its cross-validation in three test areas using a frequency ratio model. *Photogrammetrie-Fernerkundung-Geoinformation*. 2010(1):17-32.
- Pradhan, A.M.S., and Kim, Y.T. 2016. Evaluation of a combined spatial multi-criteria evaluation model and deterministic model for landslide susceptibility mapping. *Catena*. 140, 125-139.
- Pradhan, A.M.S., and Kim, Y.T. 2014. Relative effect method of landslide susceptibility zonation in weathered granite soil: a case study in Deokjeok-ri Creek, South Korea. *Natural Hazard*. 72, 1189-1217.
- Ramli, M.F., Yusof, N., Yusoff, M.K., Juahir, H., and Shafri, H.Z.M. 2010. Lineament mapping and its application in landslide hazard assessment: a review. *Bulletin of engineering Geology and the Environment*. 69(2), 215-233.
- Regmi, A.D., Devkota, K.C., Yoshida, K., Pradhan, B., Pourghasemi, H.R., Kumamoto, T., and Akgun, A. 2014. Application of frequency ratio, statistical index, and weights-of-evidence models and their comparison in landslide susceptibility mapping in Central Nepal Himalaya. *Arabian Journal of Geosciences*. 7(2), 725-742.
- Roodposhti, M.S., Rahimi, S., and Beglou, M.J. 2014. Promethee II and fuzzy AHP: an enhanced GIS-based landslide susceptibility mapping. *Natural Hazards*. 73(1), 77-95.
- Saaty, T.L. 1977. A scaling method for priorities in hierarchical structures. *The Journal of Mathematical Psychology*. 15:231-281
- Saaty, T.L. 1990. How to make a decision: the analytic hierarchy process. *The European Journal of Operational Research*. 48(1), 9-26.
- Saaty, T.L. 2005. *Theory and application of the analytic network process*. Pittsburg: RWS
- Saklani, P. 2008. Forest fire risk zonation, a case study Pauri Garhwal, Uttarakhand, India [MSc thesis]. International Institute for Geo-information Science and Earth Observation Enschede of the Netherlands and Indian Institute of Remote Sensing (NRSA) Dehradun India; p. 71.
- Sarda, V.K., and Pandey, D.D. 2019. Landslide susceptibility mapping using information value method. *Jordan Journal of Civil Engineering*, 13(2), 335-350.
- Sengupta, A. Gupta, S., and Anbarasu, K. 2010. Rainfall thresholds for the initiation of the landslide at Lanta Khola in north Sikkim, India. *Natural Hazards*. 52(1), 31-42.
- Sidle, R.C. and Ochiai, H. 2006. Landslides Processes, Prediction, and Land Use Water Resources Monograph 18. In *Natural Resources Forum* (31: 322-326).
- Skilodimou, H.D., Bathrellos, G.D., Koskeridou, E., Soukis, K., and Rozos, D. 2018. Physical and anthropogenic factors related to landslide activity in the Northern Peloponnese, Greece. *Land*. 7(3), 85.
- Stanley, T., and Kirschbaum, D.B. 2017. A heuristic approach to global landslide susceptibility mapping. *Natural Hazards*. 87(1), 145-164.
- Vakhshoori, V., and Zare, M. 2016. Landslide susceptibility mapping by comparing weight of evidence, fuzzy logic, and frequency ratio methods. *Geomatics, Natural Hazards, and Risk*. 7(5), 1731-1752.
- Varnes, D.J. 1984. *Landslide hazard zonation: a review of principles and practice*. UNESCO Press, Paris.
- Vergani, C., Chiaradia, E.A., and Bischetti, G.B. 2012. Variability in the tensile resistance of roots in Alpine forest tree species. *Ecological Engineering*. 46, 43-56
- Wilson, J.P., and Gallant, J.C. (Eds.). 2000. *Terrain analysis: principles and applications*. John Wiley & Sons.
- Xing, A.G., Wang, G., Yin, Y.P., Jiang, Y., Wang, G.Z., Yang, S.Y., and Dai, J.A. 2014. Dynamic analysis and field investigation of a fluidized landslide in Guanling, Guizhou, China. *Engineering geology*. 181, 1-14.



- Yilmaz, I. 2009. Landslide susceptibility mapping using frequency ratio, logistic regression, artificial neural networks and their comparison: a case study from Kat landslides (Tokat-Turkey). *Computers and Geosciences*. 35(6), 1125-1138.
- Youssef, A.M., Pourghasemi, H.R., Pourtaghi, Z.S., and Al-Katheeri, M.M. 2016. Landslide susceptibility mapping using random forest, boosted regression tree, classification and regression tree, and general linear models and comparison of their performance at Wadi Tayyah Basin, Asir Region, Saudi Arabia. *Landslides*, 13(5), 839-856.

